25th ABCM International Congress of Mechanical Engineering
October 20-25, 2019, Uberlândia, MG, Brazil

COB-2019-2254
PARAMETERIZATION AND EXPERIMENTAL CONTROL OF A MINI QUADCOPTER

Marcela Coury Pinto
Gabriela Vieira Lima
Gabriel Felipe Vieira de Sousa
Mariana Korndörfer dos Santos
Rafael Monteiro Jorge Alves de Souza
Aniel Silva de Morais

Federal University of Uberlândia, Department of Electrical Engineering, Uberlandia, Brazil.
Automation, Electronic Systems and Control Laboratory (LASEC)
marcelacouryp@hotmail.com; gabriela.lima@ufu.br; gabrielfelipe@ufu.br; mariana.k@hotmail.com; rafael.mjas@gmail.com; aniel@ufu.br.

Abstract. *This paper presents the development of experiments to obtain the physical parameters of a mini quadcopter. In addition, the vehicle's regulatory control will be presented through a PID control strategy. In order to validate the parameterization tests, the acquired data will be compared with the results available in the literature. Allied to this, a comparison will be made between the flights in simulated environment with the experimental tests of a real vehicle. The quadcopter used is Crazyflie 2.0, produced by Bitcraze.*

Keywords: *Crazyflie, Quadcopter, Modelling, Parameterization, Control.*

1. INTRODUCTION

Man's curiosity and persistence in discovering how animals fly has led him to the creation of airplanes, helicopters and various means of air transport.

The last decade witnessed the evolution of unmanned aerial vehicles, also known as UAV's. These vehicles have been gaining prominence due to their wide applications in civil and military areas, which has motivated researchers around the world (Xiu et al., 2017).

The quadcopter belongs to a class of unmanned aerial vehicles with rotating wings. The system is similar to a traditional helicopter, but with four sets impeller/propeller, as illustrated in Fig. 1. This aircraft has become important because of advantages such as Vertical Take-off and Landing (VTOL) as well as hovering at a certain altitude (Raffo, 2011).

Figure 1. Crazyflie 2.0.

The main disadvantage of the quadcopter is the fact that most of the prototypes use electric motors powered by batteries, in which the ratio between the amount of charge stored by the mass is relatively small (Huggins, 2008).

The control system for such vehicles is not trivial. The UAVs are non-linear, underactuated, have a time-varying behavior, and are constantly affected by aerodynamic disturbances.

In this context, this work aims to determine the physical parameters of a quadcopter, and to develop strategies for control of the aircraft, both for the model in simulation and for the real model. For this, simulations, experiments and comparisons were carried out, in order to validate the research. In this study, it was used the Crazyflie Quadcopter 2.0, produced by Bitcraze.

2. DYNAMIC MODELLING

The dynamic model of the system is based on the following hypotheses:

(a) The structure of the aircraft is considered rigid and symmetrical;
(b) The vehicle's center of mass coincides with the origin of the fixed coordinate system to the rigid body;
(c) The propellers are considered rigid;
(d) The thrust and drag are proportional to the square of the speed of the propellers.

The generalized coordinates of a rigid body in three-dimensional space can be defined as:

$$q = [x \quad y \quad z \quad \phi \quad \theta \quad \psi] \tag{1}$$

where, $[x \quad y \quad z]$ is the position of the center mass of the quadrotor in relation to the inertial system (*I*) and $[\phi \quad \theta \quad \psi]$ represent the Euler angles describing the orientation of the aerial vehicle in three-dimensional space.

The quadcopter operates through the variation of the angular velocity of four motors, in such a way that each motor produces a force and a torque, and when combined, generate a thrust and three torques (roll, pitch and yaw).

The electric motors operate with a fixed rotation sense, therefore, the force generated by each motor is always positive. To avoid the use of a tail rotor, each motor has a defined sense of rotation: the front (M1) and rear (M3) rotate counterclockwise, while the left (M2) and right (M4) operate clockwise, as shown in Fig. 2.

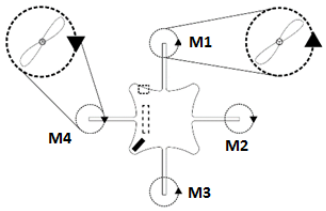

Figure 2. Schematic diagram of a quadrotor.

Based on the concepts of kinetic and potential energy, it is possible to determine the dynamic equations through the Euler-Lagrange formalism, represented by Eq. (2):

$$\begin{bmatrix} f_\xi \\ \tau_\eta \end{bmatrix} = \frac{d}{dt}\left(\frac{\partial L}{\partial \dot{q}_i}\right) - \frac{\partial L}{\partial q_i} \qquad L(q,\dot{q}) = E_{KT} + E_{KR} - E_P \tag{2}$$

Where *L* is the Lagrangian, E_{KT} and E_{KR} are the kinetics energy and E_p represents the potential energy. The applied translational force in the aircraft is characterized by f_ξ and $\tau = [\tau_\phi \quad \tau_\theta \quad \tau_\psi]$ defines the moments of roll, pitch and yaw.

The development of the equations of motion has already been performed (Lima, 2015), and the dynamic referring to the translational subsystem is presented in Eq. (3):

$$\begin{cases} \ddot{x} = \frac{1}{m}\left(\cos\psi\, sen\theta\, \cos\phi + sen\psi\, sen\phi\right)U_1 \\ \ddot{y} = \frac{1}{m}\left(sen\psi\, sen\theta\, \cos\phi - \cos\psi\, sen\phi\right)U_1 \\ \ddot{z} = -g + \frac{1}{m}\left(\cos\theta\, \cos\phi\right)U_1 \end{cases} \tag{3}$$

where m is the total mass of the quadrotor, g represents gravitational acceleration and U_1 is the thrust.

The dynamic equations of the rotational subsystem can be defined according with the Eq. (4), where b is the thrust coefficient, *d* is the drag coefficient, *l* is the distance from the center of mass to the axis of the motors, Ω_i is the angular velocity of each motor around its axis and I_{ii} are the components of the inertia matrix.

$$\begin{cases} \ddot{\phi} = \dfrac{(I_{yy} - I_{zz})\dot{\theta}\dot{\psi}}{I_{xx}} + \dfrac{bl/\sqrt{2}\,(-\Omega^2_1 - \Omega^2_2 + \Omega^2_3 + \Omega^2_4)}{I_{xx}} \\ \ddot{\theta} = \dfrac{(I_{zz} - I_{xx})\dot{\phi}\dot{\psi}}{I_{yy}} + \dfrac{bl/\sqrt{2}\,(-\Omega^2_1 + \Omega^2_2 + \Omega^2_3 - \Omega^2_4)}{I_{yy}} \\ \ddot{\psi} = \dfrac{(I_{xx} - I_{yy})\dot{\theta}\dot{\phi}}{I_{zz}} + \dfrac{d(\Omega^2_1 - \Omega^2_2 + \Omega^2_3 - \Omega^2_4)}{I_{zz}} \end{cases} \quad (4)$$

3. PARAMETERIZATION

The parameters analyzed in the aircraft were mass, distance between the center of mass and the rotors (half wingspan), thrust coefficient, moment of inertia, and drag coefficient.

3.1 Mass

The mass of the quadcopter was measured through a scale with a maximum capacity of 220 g and an accuracy of 0.0001 g. Crazyflie 2.0 consists of a control board, one 240mAh LiPo battery, four DC coreless motor with motor mounts, one battery holder deck and four propellers. The total mass of Crazyflie 2.0 is 28.2844 grams, each measure is represented in Tab. 1.

Table 1. Crazyflie mass.

Parameter Description	Mass (g)
Crazyflie 2.0 control board	6.7307
240mAh LiPo battery	7,1667
DC coreless motor	2.5768
Motor support	0.3922
Battery holder deck	1.4418
Propellers	0.2673
Total	**28.2844**

3.2 Half wingspan

To measure the half wingspan, it was used an analog caliper with an accuracy of 0.05 mm. The length related to both x-axis and y-axis is 0.0461 m and the length related to z-axis is 0.0123 m.

3.3 Thrust coefficient

Thrust is the aerodynamic force produced by a turbine or propeller. The thrust force is responsible for the upward and downward movement of the quadcopter, and corresponds to the sum of the individual forces generated by each motor (Lima, 2015).

In this experiment, the following equipment's were used: a 0,01 g precision scale with a maximum capacity of 500 g, bottle of water, Crazyflie 2.0, adhesive tape, reflective tape and a tachometer. The optical tachometer was used to measure the angular velocity of the motors (RPM) and the electronic scale to quantify the force produced. The motor power was increased in 16 steps, changing the duty cycle (PWM) value from 0% to 93.75%. The thrust value was measured 3 times for each step and averaged. The data was analyzed in Matlab software, and the result is presented in Tab. 2.

It has been observed during the tests that it is necessary to use a balance with contact surface approximately the size of the bottom of the bottle. Otherwise, the force of the airflow underneath the quadcopter exerts force on the measuring surface of the balance and interferes with the results. Figure 3 represents the experiment.

Figure 3. Thrust coefficient test.

Table 2. Result of the thrust coefficient.

Thrust (g)	Duty Cycle (%)	Velocity (RPM)
0.00	0.00	0.00
1.60	6.25	4804.33
5.10	12.50	7643.67
8.20	18.75	9796.00
11.90	25.00	11177.33
15.20	31.25	12134.67
18.10	37.50	12871.00
21.90	43.25	12945.00
25.30	50.00	15349.00
28.00	56.25	15990.33
31.10	62.50	16330.67
34.75	68.75	16840.00
39.70	75.00	19304.33
42.75	81.25	19910.00
46.45	87.50	20035.33
49.90	93.75	20449.00

Figures 4 and 5 show the relationship between the thrust values with the duty cycle (PWM) and velocity (RPM), respectively. The curves were obtained through the polyfit function of MATLAB.

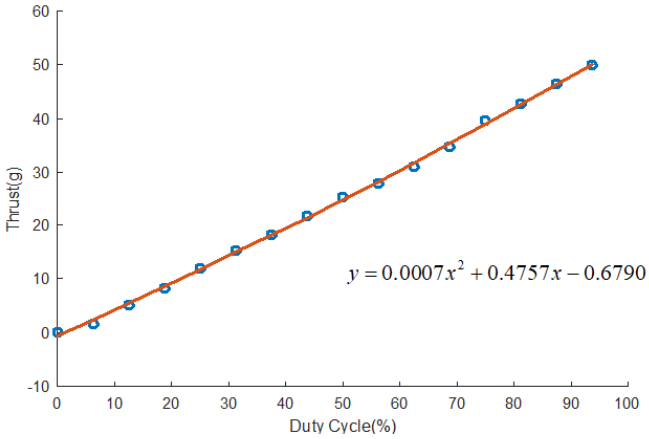

Figure 4. Thrust vs Duty Cycle.

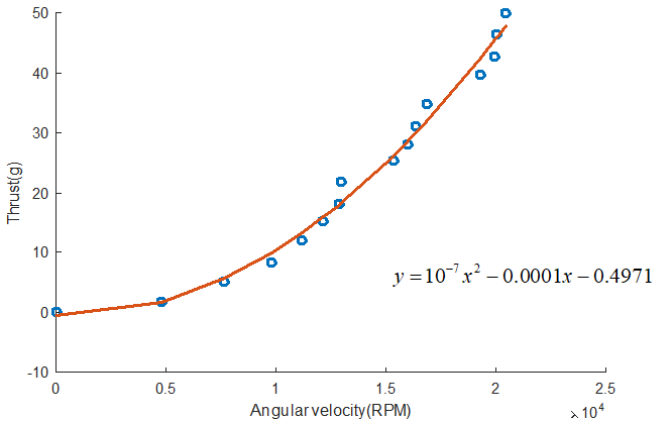

Figure 5. Thrust vs Velocity.

To obtain the thrust coefficient it is necessary to convert the mass to the international system and then divide by the angular velocity as in the Eq. (5).

$$F = b\Omega^2 \tag{5}$$

The results obtained for the thrust coefficient were:

- By the data acquisition: $2.3646 \cdot 10^{-8} kg \cdot m / rad^2$
- By adjusting curves: $2.3933 \cdot 10^{-8} kg \cdot m / rad^2$

Comparing the values of the data collected with those of the curve fitting it is possible to verify that they are close, therefore the team will use the values of the thrust coefficients for the data acquisition.

3.4 Moment of inertia

The moment of inertia expresses the degree of difficulty in changing the motion state of a rotating body, in other words, it is the resistance to the angular velocity change. In the calculation was used Computer-aided design (CAD) and SolidWorks software. In this software it is necessary to open the tab "Property of mass" and enter the values of each component in its due space. CAD must be in the form of the quadcopter, although, it does not have to contain every detail of the vehicle. The model used can be found in GitHub (Shu, 2017) and is shown in Fig. 6. The results of the simulation are presented in Tab. 3.

Figure 6. SolidWorks model.

3.5. Drag coefficient

The drag coefficient is used to model all the complex dependencies of shape, inclination, and flow conditions on aircraft drag (Hall, 2015). This parameter was calculated using SolidWorks software, with the same 3D model used for the moment of inertia, associated with the Flow Simulation. The result is shown in Tab. 3.

The dimensionless drag coefficient is given by the Eq. (6).

$$C_d = \frac{F_d}{(0.5V^2 A\rho)} \tag{6}$$

Where:

F_d - Drag force;

V - Wind speed;

A - Surface area of the aircraft in contact with the wind;

ρ - Fluid density.

The simulation in SolidWorks is presented in Fig. 7.

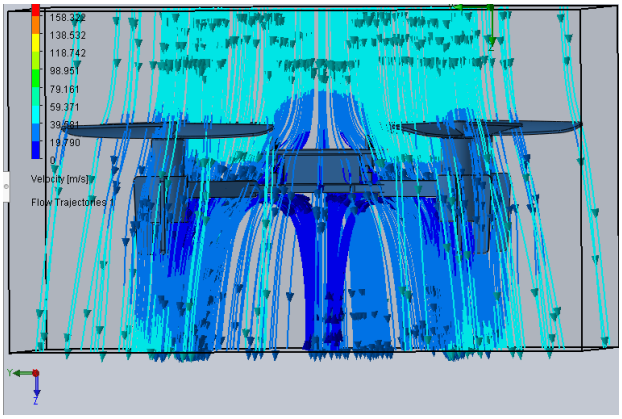

Figure 7. Drag simulation.

In the simulation was used $V = 45.535 \ \ m/s$ and $\rho = 1.29 \ \ kg/m^3$. The result was: $C_d = 0.2056$.

As the program provides the value of the dimensionless drag coefficient, it is necessary to convert this value to kgm^2/rad^2 to use in the comparison. With the previously values it is possible to calculate the drag coefficient, as shown in the Eq. (7) (Bouabdallah and Siegwart, 2007).

$$d = C_p r^3 A \rho \tag{7}$$

Table 3. Crazyflie parameters.

Parameter Description	Symbol	Unit	Value
Mass	m	kg	$28.2844 \cdot 10^{-3}$
Half Wingspan	l	m	0.0461
X-axis Inertia	I_{xx}	$kg \cdot m^2$	$1.4730 \cdot 10^{-5}$
Y-Axis Inertia	I_{yy}	$kg \cdot m^2$	$1.4797 \cdot 10^{-5}$
Z-axis Inertia	I_{zz}	$kg \cdot m^2$	$2.8476 \cdot 10^{-5}$
Thrust Coefficient	b	$kg \cdot m / rad^2$	$2.3646 \cdot 10^{-8}$
Drag Coefficient	d	$kg \cdot m^2 / rad^2$	$1.2171 \cdot 10^{-10}$

4. CONTROL STRATEGY

As shown by Eq. (3) e (4), the angles and their time derivatives do not depend on the translational components. On the other hand, the translational system depends on the angular coordinates. Therefore, it is convenient to adopt a cascade control model, as represented in the Fig. (8).

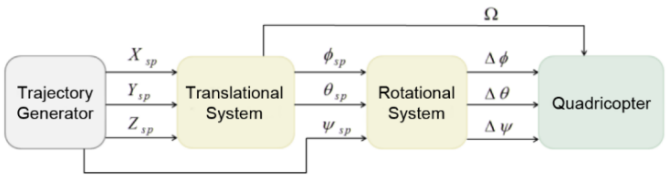

Figure 8. Schematic of the control strategy.

The rotational subsystem corresponds to the internal loop and regulates the orientation of the aircraft. The translational subsystem corresponds to the external loop and controls the linear speed and position of the vehicle.

The discrete PID controller expression used in quadrotor control is presented in Eq. (8):

$$\begin{cases} P_k = K_p e_k \qquad I_k = I_{k-1} + K_i T_s e_k \qquad D_k = K_d \dfrac{(e_k - e_{k-1})}{T_s} \qquad u_k = P_k + I_k + D_k \end{cases} \tag{8}$$

where K_p is the proportional gain, K_i represents the integral gain, K_d defines the derivative gain, T_s is the sampling time, e_k is the error signal and u_k represents the output signal of the controller.

The control was implemented with the aid of a base station (computer), through a routine in Scilab software (where the translational compensator calculations were carried out) in parallel to a Python script (where the setpoint was set). The manufacturer implemented the protocol of radio communication.

The controllers were tuned by means of empirical methods followed by fine-tune. The gains were analyzed through simulations, and then validated in the experimental system. The values obtained are presented in Tab. 4.

Table 4. Compensator gains.

Control	K_p	K_i	K_d
X	3.5	0.0	0.3
Y	3.5	0.0	0.3
Z	1.8	0.7	0.2
$\dot{X}$	35.0	10.0	0.0
$\dot{Y}$	35.0	10.0	0.0
$\dot{Z}$	25.0	15.0	0.0
ϕ	8.0	3.0	0.0
θ	8.0	3.0	0.0
ψ	4.0	1.0	0.35
$\dot{\phi}$	250.0	500.0	2.5
$\dot{\theta}$	250.0	500.0	2.5
$\dot{\psi}$	120.0	16.7	166.7

5. RESULTS

The results were analyzed comparing experimental tests and simulations in a computational environment. The simulations were performed in Scilab 6.0.1. It is important to note that in the simulation, the linear controller was applied to the nonlinear model.

A regulation problem is presented below, where some setpoints have been set in step and the aircraft must maintain its constant position. Figure 9 shows the system response to the translational coordinates.

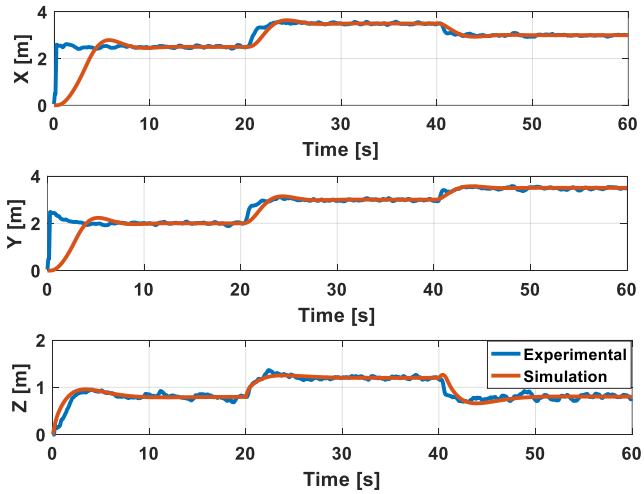

Figure 9. System responses to the translational coordinates.

Comparing the simulation with the experimental test it is possible to observe that for the X and Y coordinates, the response in a computational environment tends to exhibit a longer accommodation time. In contrast, for the Z coordinate, in a few moments the simulation is slightly faster. In addition, no steady-state error and no overshoot is observed in the X and Y coordinates.

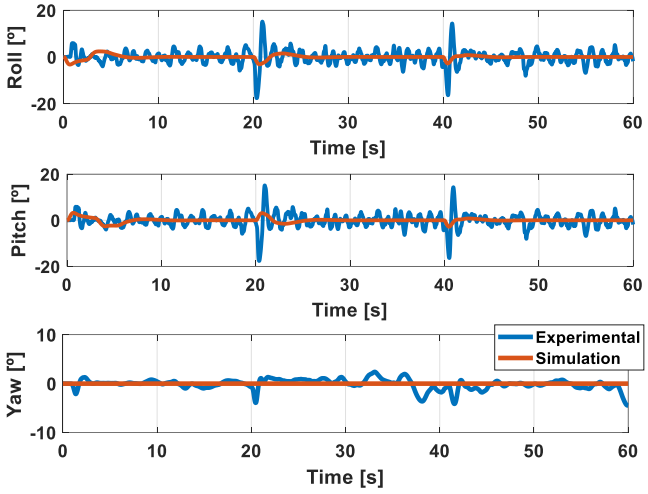

Figure 10. System responses to the rotational coordinates.

The angular coordinate responses present peaks at the setpoint transition points. At steady state, the oscillations for the roll and pitch angles have an average amplitude of five degrees, while for the yaw angle, it is approximately two degrees. It should be noted that the reference of the yaw angle is zero, so that the quadrotor cannot rotate around the z-axis.

It should be emphasized that the roll, pitch and yaw angles should have small values. In the event of disturbances that lead to high angular inclinations (greater than 20º), the system will operate in a region where nonlinearities become more relevant and, consequently, the essentially linear PID controller fails to stabilize the aircraft.

6. CONCLUSION

In this paper, the experiments to obtain the physical parameters of the quadcopter Crazyflie 2.0 were presented, besides the development of a strategy of a PID controller for the flight of the aircraft. Data from the simulation and the real vehicle make it possible to verify that the values obtained for the physical parameters are promising. In addition, it was possible to verify that the PID controller is well tuned, since it can follow the setpoint change and has stability. The positioning system was able to provide good results as well.

Further works will notably focus on development of the multi-aircraft cooperation algorithm as well as the trajectory tracking performed by a camera coupled in each vehicle, which will allow flights in unknown environments.

7. REFERENCES

Bouabdallah, S. and Siegwart, R., 2007. “Full Control of a Quadrotor”, in Proc. IEEE IROS, USA, pp. 153–158.
Hall N., 2015. “The Drag Coefficient”. National Aeronautics and Space Administration.

Raffo, G. V., “Robust Control Strategies for a Quadrotor Helicopter: An Underactuated Mechanical System”, Ph.D. dissertation, Depto. De Ingeniería de Sistemas y Automática, Universidad de Sevilla, Sevilla, Spain, 2011.

Huggins, R. A, 2008. Advanced Batteries : Materials Science Aspects, SpringerLink : Springer e-Books, Springer. URL : http://books.google.com.br/books?id=atEOtixRHvcC

Landry, B. , 2015. "Planning and Control for Quadrotor Flight through Cluttered Environments",Massachusetts Institute of Technology.

Lima, G. V., 2015. "Modelagem dinâmica e controle para navegação de um veículo aéreo não tripulado do tipo quadricóptero". Master's thesis, Universidade Federal de Uberlândia, Uberlândia, 119 f.

Lowara, 2003. “Bitcraze”. Jun, 2018 < https://www.bitcraze.io/crazyflie-2/>.

Mcinerney, I. , 2017. "Development of a multi-agent quadrotor research platform with distributed computational capabilities", Iowa State University, Ames, Iowa.

Shu, R., 2017. “3D CAD Model of Crazyflie Quadrotor”. Jun, 2018 < https://github.com/rshum19/Crazyflie-CAD>.

Xiu, H., Xu, T., Jones, A., Wei, G. and Ren, L, 2017. "A reconfigurable quadcopter with foldable rotor arms and a deployable carrier," IEEE International Conference on Robotics and Biomimetics (ROBIO), Macau, pp. 1412-1417.

8. RESPONSIBILITY NOTICE

The authors are the only responsible for the printed material included in this paper.